
STUDY OF CONDITIONS FOR HIERARCHICAL CONDENSATION NEAR THE PHASE EQUILIBRIUM

O.I. OLEMSKOI,¹ O.V. YUSHCHENKO,² T.I. ZHYLENKO²

¹**Institute of Applied Physics, Nat. Acad. of Sci. of Ukraine**
(58, Petropavlivska Str., Sumy 40030, Ukraine)

²**Sumy State University**
(2, Rymskyi-Korsakov Str., Sumy 40007, Ukraine; e-mail: alex@ufn.ru)

PACS 05.65.+b, 81.15.Aa
©2011

A new mechanism of phase formation has been proposed and studied, both experimentally and theoretically, using quasiequilibrium stationary condensation in an ion-plasma atomizer as an example. Copper condensates were obtained, which testifies that a self-assembling mode is realized in the course of sputtering, giving rise to the appearance of a characteristic grid structure. The obtained fractal pattern of the condensate nucleus distribution over the substrate surface is similar to that observed in the course of diffusion-limited aggregation. The condensate nuclei were shown to form a statistical ensemble of hierarchically constrained objects distributed in an ultrametric space. The Langevin and Fokker-Planck equations describing the behavior of this ensemble were derived, which allowed the stationary distribution of thermodynamic condensation effect values and the corresponding probability flow to be determined. The time dependences for the formation probability of branched condensate structures are obtained, which allowed the formation of the grid structure to be explained.

1. Introduction

The development of the condensation considered as a phase transition of the first kind may follow either the spinodal or binodal mechanism [1, 2]. In the former case where the deposited vapor is thermodynamically unstable, the condensate is formed due to an increase of homogeneous fluctuation amplitudes. In the binodal region of the phase diagram, where the vapor and the condensate may coexist, the evolution of the system is reduced to the size growth of heterogeneous fluctuations, which represent nuclei of the condensed phase. Under real experimental conditions, the condensation centers arise in the form of monobends on steps of the growth surface, inhomogeneities on an atomically rough surface, the sites of crystallite splicing, and so on. Therefore, the spinodal mechanism of homogeneous condensation turns out, as a rule, impossible, and the latter scenario is realized, which is known as the classical mechanism of phase nucleation and growth.

In the general case, this scenario is reduced to the following stages [3]. First, the fluctuation formation of nuclei takes place, when the nuclei overcome the critical dimension $R_c \sim \sigma/\Delta f$ determined by the coefficient of surface tension σ . The latter is equal to the difference Δf of phase free energies in a unit volume, which is proportional, in turn, to the difference $n - n_e$ between the concentration of deposited atoms n and the equilibrium value n_e . If the initial concentration n_{in} is so high that $n_{in} \gg n_e$, then, in spite of a permanent drift of nuclei in the supercritical region, $R > R_c$, the growth of precipitations occurs already at a concentration $n(t) \approx n_{in}$, which is practically identical to the initial value. At the subsequent condensation, the deposited vapor becomes exhausted, when its concentration n becomes comparable with the equilibrium value n_e . This provides an exponentially rapid decrease of oversaturation $n - n_e$, and the critical radius $R_c \propto (n - n_e)^{-1}$ reaches the value of R_g , the limiting dimension of a region accounted for one precipitation. At this stage, the majority of precipitations have supercritical dimensions, $R > R_c$, and their number remains almost invariable. Starting from the time moment, when the condition $R_c(t) \sim R_g$ is satisfied, precipitations begin to come back from the supercritical region, $R > R_c$, into the subcritical one, $R < R_c$, following the Lifshitz-Slyozov mechanism of coalescence, when larger precipitations grow at the expense of small ones [4]. In this case, the critical radius grows according to the power law $R_c^p \propto t$ with the exponents $p = 2, 3, \text{ or } 4$; the specific value being determined by the mechanisms of atomic transfer between precipitations [5].

This scenario manifests itself, when various nanosystems are formed in the course of condensation, which can be realized owing to the wide application of modern technologies, such as molecular beam epitaxy, electrolytic deposition, liquid phase epitaxy, and so forth [6]. A specific feature of the mentioned technologies is that their application provides a stationary development of the condensation at the oversaturation $n - n_e \ll n_e$, the

low values of which mean the proximity of the plasma–condensate system to the phase equilibrium. As a result, the critical radius $R_c \propto (n - n_e)^{-1}$ turns out so large that the fluctuation formation of nuclei becomes almost impossible.

In a number of indicated technologies, it is necessary to single out the experimental technique [7–11], in which quasiequilibrium conditions of condensation are reached in a self-organized manner. The heating of the growth surface by a plasma flux ensures that the oversaturation is extremely low and permanent in the course of sputtering. As a result, the adsorbed atoms become fixed on the growth surface only if they engage the strongest chemical bonds.

In contrast to the techniques used in works [6–11], an experimental procedure of quasiequilibrium surface condensation was applied in work [12]. The procedure is based on standard plasma technologies [13, 14]. In its framework, the proximity to the phase equilibrium in the vapor–condensate system is achieved owing to the extreme weakening of a deposited flux in combination with the elevated temperature of the sputtered surface and the high pressure of the preliminarily purified working gas. Such conditions allowed the process of hierarchical condensation to be implemented. The corresponding picture of phase growth reminds the formation of a percolation cluster at the flow of a liquid through a medium with a random structure [15].

This work is devoted to the study of hierarchical condensation conditions implemented in work [12]. In Section 2, a short description of experimental conditions, under which the process of hierarchical condensation was managed to be carried out, is given. It is shown that a grid structure – a result of the hierarchical condensation – is formed on the substrate at a low concentration of condensation centers. Section 3 is devoted to the parametrization of the process of such a condensation on the basis of the assumption that the condensate nuclei correspond to nodes in a hierarchical tree. In Section 4, a statistical scenario is expounded, in the framework of which the process of hierarchical condensation is regarded as a diffusion process in an ultrametric space that parametrizes the fractal structure obtained. The distributions of condensate nuclei over the energies of their formation and the hierarchical levels have been found. In Section 5, they are used as a basis for the determination of time dependences for the formation probabilities of hierarchical structures with different branching degrees. The final section 6 compares experimental data [12] and the results of the developed theoretical scheme. Details concerning the cal-

culaton of a hierarchical condensation probability with the use of the saddle-point method are presented in Appendix.

2. Experimental Procedure and Results Obtained

Superfine copper condensates were studied. They were sputtered in a planar dc magnetron atomizer with the discharge power lowered from usual 50–100 to 2.5–4 W [12]. Such a reduction allowed the deposited flux to be diminished to threshold values, which provide the condensate formation. As a working gas, we used argon, the pressure of which was raised from 1 to 10 Pa. The vacuum chamber was equipped with an MX7304A mass-analyzer with a sensitivity not worse than 10^{-12} Pa. The partial pressure of chemically active residual gases was reduced to 8×10^{-8} Pa by sputtering titanium from auxiliary magnetrons located over the vacuum chamber [16]. The substrate was heated up to 650 K.

The application of the device described allowed us to ensure a stable mode of quasiequilibrium sputtering. As was already mentioned, it was attained by using an extremely low deposition flux and an elevated temperature of the substrate. On the other hand, an increase of the working gas pressure results in strengthening the collisions between plasma particles, which gives rise to a narrowing of their energy spread [14] and favors the uniform distribution of a sputtered substance over different facets of the crystal growth surface.

Condensation occurred in the Folmer–Weber regime on as-cleaved facet (001) surfaces of KCl substrates. As was pointed out in Introduction, the condensation process in a vicinity of the phase equilibrium is possible only provided that there are active centers of crystallization with increased chemical bond energies. The role of such centers on the KCl substrate is played by Cl^- vacancies, the formation of which is ensured by the influence of a flux of secondary electrons emitted by the magnetron atomizer [13].

The obtained copper condensates were fixed by depositing amorphous carbon layers. Afterwards, KCl substrates were washed out in a water stream. The structure and the phase composition were determined making use of electron diffraction analysis and by analyzing the microdiffraction of high-energy electrons.

Electron microscopy patterns of copper condensates, which are shown in Fig. 1, illustrate the evolution of their cluster structure in the course of sputtering. According to Fig. 1, *a*, isolated clusters are formed at the initial stage. Every cluster consists of a number of con-

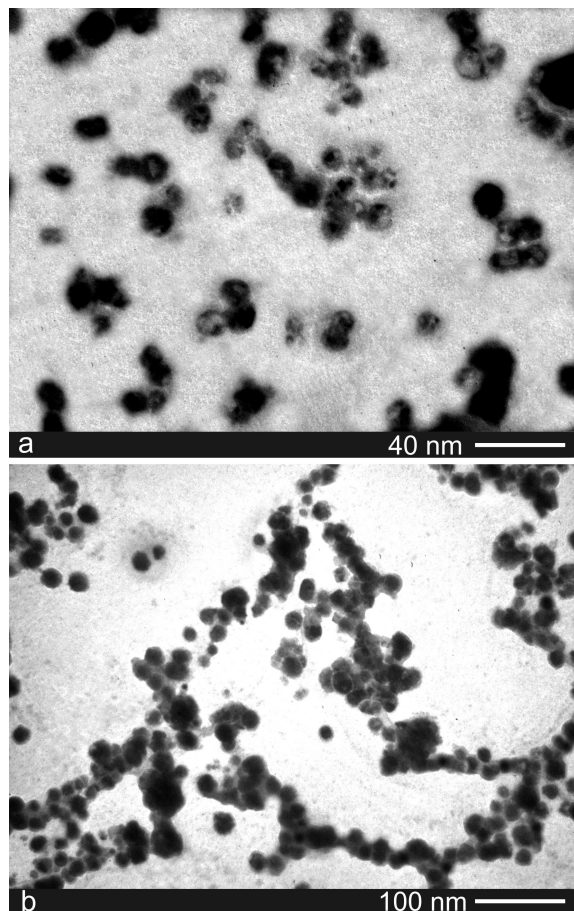


Fig. 1. Electron-microscopy patterns of copper condensates grown up *ex-situ* during (a) 6- and (b) 14-min sputtering

densate nuclei. In due course, a secondary nucleation of precipitations takes place near the initial clusters, the boundaries of which play the role of crystallization centers. Figure 1,*b* demonstrates that the most effective centers of secondary condensation are single phase nuclei. Therefore, they arranged into branched chains in the course of sputtering, which means the self-assembling of a condensate grid structure. It is characteristic that such a behavior manifests itself only at a low concentration of crystallization centers on the substrate.

3. Parametrization of Hierarchical Condensation Process

The presented experimental data testify to the hierarchical origin of the condensation process. First, the small clusters of phase nuclei are formed at the crystallization centers on the substrate. Then, their boundaries serve as a place for the secondary condensation, and the

process repeats over and over again. As a result, a characteristic grid structure is formed. It is similar to the structure, which is observed in the course of diffusion-limited aggregation. In this case, the condensate forms a fractal structure, which is similar to percolation clusters observed at a liquid flow through a random medium [15]. In what follows, we shall demonstrate that hierarchical structures of this kind are formed as a result of the diffusion process in a hypothetical space, which has an ultrametric topology (it is pertinent to call this space ultrametric) [17].

While developing the proposed scenario, it is possible to identify every nucleus in the condensate with a node in the hierarchical tree and to present the clusterization process as a motion of a configuration point from the lowest (the most branched) levels to the tree root. Let us consider firstly the node distributions over the hierarchical levels for various trees [18].

Let the maximal number of nodes, N , be located at the lowest level and correspond to the distance $s = 0$ in the ultrametric space. This level is associated with a complete ensemble of individual nuclei, the number of which, N , coincides with the number of nodes. The top level of the hierarchical tree contains a single node, which corresponds to the common cluster of all nuclei and is characterized by the distance maximum $s = S \gg 1$. The problem is reduced to the determination of the dependence $N(s)$, which gives the distribution of tree node numbers over the hierarchical levels.

Before proceeding to the solution of the problem, let us consider the basic types of hierarchical trees depicted in Fig. 2: a regular tree with a branching degree $b > 1$; the Fibonacci tree with $b \approx 1.618$; a degenerate tree, with only one branching node at every level; and a random tree, the main object of our consideration. Let the number l enumerate the hierarchical levels in such a manner that its minimal value corresponds to the tree top, and the maximal one, $l = S$, to the lowest level. Then, the variable

$$s = S - l \quad (1)$$

determines a distance in the ultrametric space, the points of which correspond to the nodes in the Cayley tree of the type shown in Fig. 2. Distance (1) between the nodes at a given level is defined at that by the number of steps to their mutual ancestor, and the transition to the continuum space is provided by the limits $b, S \rightarrow \infty$ [17].

As Fig. 2,*a* demonstrates, in the simplest case of a regular tree that is characterized by an integer branching degree b , the node number, $N_l = b^l$, falls down

exponentially as the distance s between nodes grows: $N(s) = N \exp(-s \ln b)$, where $N \equiv b^S$. For the Fibonacci tree (Fig. 2,b) – here, $N_l = \nu \tau^l$, $\nu \approx 1.171$, and $\tau \approx 1.618$ – we obtain $N(s) = N \exp(-s \ln \tau)$, where $N \equiv \nu \tau^S$. Therefore, a conclusion may be drawn that the exponential distribution of node numbers over the hierarchical levels, which is realized not only for integer, but also for fractional branching degrees, is inherent to regular Cayley trees. In the limiting case of a degenerate tree (Fig. 2,c), when $N_l = (b - 1)l + 1$, we arrive at the linear dependence $N(s) = N - (b - 1)s$, where $N \equiv (b - 1)S + 1$.

For a random tree of the type that is exhibited in Fig. 2,d, we suppose the power-law distribution

$$N_l = l^a, \quad a > 1. \tag{2}$$

It can be regarded as an intermediate case between the exponential and linear dependences, which correspond to the limiting distributions taking place in regular and degenerate trees, respectively. From a formal point of view, the power-law dependence (2) means that the function $N(x)$, which is defined on a self-similar ensemble of hierarchical objects, is homogeneous, i.e. it satisfies the condition $N(lx) = l^a N(x)$. Depending on distance (1), this means that $N(s) = N(1 - s/S)^a$, where $N \equiv S^a$ and $a > 1$.

4. Statistical Picture of Hierarchical Condensation

Consider now the statistical distribution of condensate nuclei over the absolute values F_l of free energy changes at their formation, $-F_l$, which depend on the level number l . At a given distribution F_l , the probability flow for the transition between levels l and $l + 1$, provided that $l \gg 1$, is expressed by the Onsager generalized relation

$$j_l = -m(F_l) \frac{dF_l}{dl}. \tag{3}$$

In the framework of the approach that takes the presence of the internal multiplicative noise into account, the coefficient of effective mobility,

$$m(F_l) = M F_l^\beta, \tag{4}$$

is defined in terms of the constant $M > 0$ and the index β [19]. Under stationary conditions where the total flow does not depend on the hierarchical level number,

$$j_l N_l = \text{const} \equiv J, \tag{5}$$

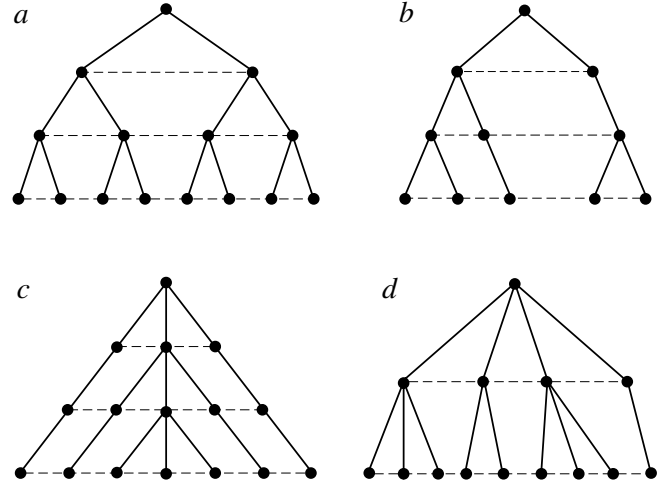


Fig. 2. Basic types of hierarchical trees: (a) a regular tree with the branching index $b = 2$, (b) the Fibonacci tree; (c) a degenerate tree with the branching index $b = 3$; (d) a random tree with the distribution $N_l = l^2$ of the node number over the levels

the substitution of equalities (2)–(4) into Eq. (5) gives rise to the scaling relation

$$F_l = N^{\alpha/a} l^{-\alpha} f_l \tag{6}$$

with the index

$$\alpha = \frac{a - 1}{1 + \beta} > 0. \tag{7}$$

The slowly varying multiplier f_l is determined by the effective equation of motion

$$\frac{dx}{d\tau} = -\frac{\partial V}{\partial x}, \tag{8}$$

where the time, coordinate, and scale are defined by the formulas

$$\tau = \ln l^\alpha, \quad x = f_l / f_c, \quad f_c = (J / \alpha M)^{a/(a-1)} N^{-1}, \tag{9}$$

respectively. The effective potential

$$V = \frac{x^{1-\beta}}{1-\beta} - \frac{x^2}{2} \tag{10}$$

reaches its maximum value

$$V_c = \frac{1}{2} \frac{1 + \beta}{1 - \beta} \tag{11}$$

at the point $x = 1$ and monotonously falls down at $x > 1$. The dependence $F(s)$ of the thermodynamic effect of

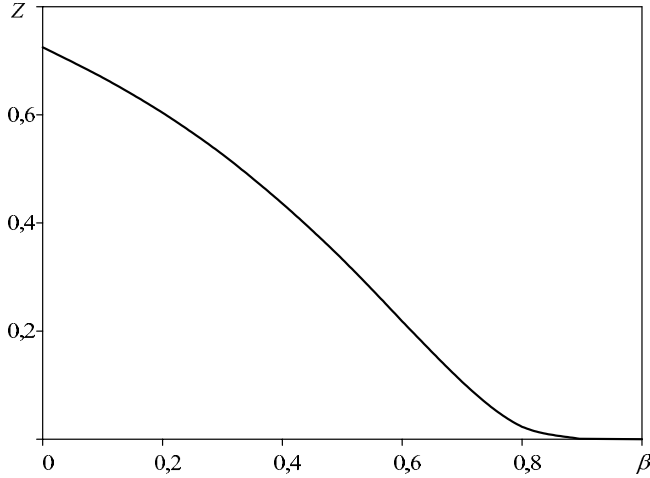


Fig. 3. Dependence of the partition function (16) on the effective mobility index (4)

condensation on distance (1) is determined by equality (6).

The corresponding consideration showed that the process of hierarchical condensation starts from the fluctuation-assisted overcoming of barrier (11) by subcritical nuclei at the lowest level, which have the specific free energy $f_l < f_c$. This process is described by the Langevin equation (cf. Eq. (8))

$$\frac{dx}{d\tau} = -\frac{\partial V}{\partial x} + \eta \tag{12}$$

with the external white noise $\eta = \eta(\tau)$ that satisfies the conditions

$$\langle \eta(\tau) \rangle = 0, \quad \langle \eta(\tau)\eta(\tau') \rangle = 2\delta(\tau - \tau'), \tag{13}$$

where the angular brackets mean the averaging. From the formal point of view, Eq. (12) describes the diffusion in the ultrametric space. The solutions of this equation compose a statistically distributed set $\{x(\tau)\}$, and the density of their realization probability is given by the function $w(\tau, x) := \langle \delta[x - x(\tau)] \rangle$. The latter is determined by the Fokker–Planck equation [20]

$$\frac{\partial w}{\partial \tau} + \frac{\partial i}{\partial x} = 0, \quad i \equiv -w \frac{\partial V}{\partial x} - \frac{\partial w}{\partial x}. \tag{14}$$

In the equilibrium state where the probability flow i equals zero, the distribution function is reduced to the Gibbs formula

$$w_0(x) = Z^{-1} \exp \{-V(x)\}, \tag{15}$$

with the effective potential (10). The partition function Z is defined by the normalization condition for subcrit-

ical nuclei, according to which

$$Z = \int_0^1 \exp \left(\frac{x^2}{2} - \frac{x^{1-\beta}}{1-\beta} \right) dx. \tag{16}$$

For distribution (15), the saddle-point method gives the estimate $Z \sim e^{-V_c}$, which includes the probability of the fluctuation-assisted overcoming of barrier (11) of the effective potential (10).

As is seen from Fig. 3, a growth of index β leads to a monotonous fall of the partition function from the value $Z \approx 0.725$ at $\beta = 0$ to $Z = 0$ at $\beta = 1$. Whence, the conclusion may be drawn that the behavior of the system concerned acquires an anomalous character as the index of effective mobility (4) increases to values $\beta \approx 1$.

In a nonequilibrium steady state, the probability density $w(x)$ does not depend on the variable $\tau = \ln l^\alpha$, which is defined by the number of a hierarchical level, and the probability flow has a constant value $i_0 \neq 0$. According to the last of Eqs. (14), the stationary, $w(f)$, and equilibrium, $w_0(f)$, distribution functions are coupled by the equality

$$\frac{w(f)}{w_0(f)} = i_0 \int_{f/f_c}^{\infty} \frac{dx}{w_0(x)}, \tag{17}$$

in which the limiting condition $w \rightarrow 0$ at $f \rightarrow \infty$ is taken into account.

Equation (17) allows the stationary flow of probability i_0 to be determined for the given thermodynamic effect f . However, one has to bear in mind in this case that the value of f is confined from below by the condition $f > G$, which makes allowance for the presence of a gap G in hierarchical ensembles [22]. Really, in the course of hierarchical condensation, not only single nuclei may play the role of elementary structural units, but their clusters composed of s nuclei, the number of which is confined by the condition $s < s_g$, where the limiting size s_g corresponds to the thermodynamical effect $G = f(s_g)$. Therefore, all clusters, for which $f < G$, should be omitted from the consideration. As a result, the stationary flow i_0 is determined by Eq. (17) together with the boundary condition $w(G) = w_0(G)$:

$$i_0^{-1} = Z \int_{G/f_c}^{\infty} \exp \left(\frac{x^{1-\beta}}{1-\beta} - \frac{x^2}{2} \right) dx. \tag{18}$$

From Fig. 4, it is evident that, as the gap is widened to the critical value $G = f_c$, the flow i_0 slowly grows,

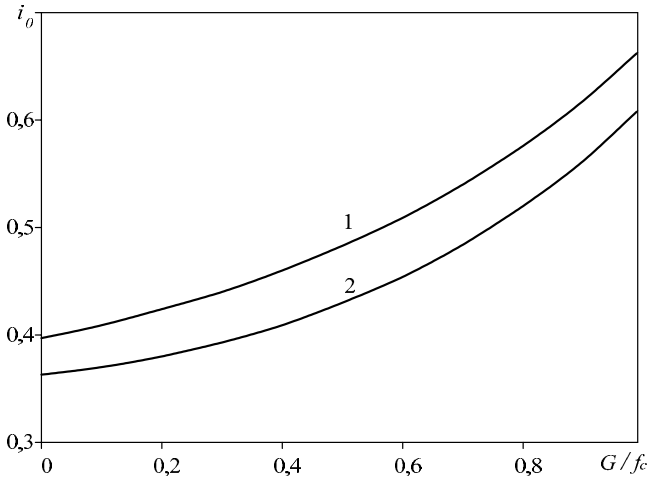


Fig. 4. Dependences of the stationary flow of probability on the gap width for the index $\beta = 0.0$ (1) and 0.5 (2)

slightly decreasing with increase in index β . At $\beta = 0$, equality (18) brings about the explicit expression

$$i_0 = I \left[1 + \operatorname{erf} \left(\frac{1 - G/f_c}{\sqrt{2}} \right) \right]^{-1}, \quad I \equiv \sqrt{\frac{2}{e\pi}} Z^{-1}. \quad (19)$$

In the general case, the flow magnitude is reciprocal to the partition function (16). Taking the relation $Z \sim e^{-V_c}$ into account, the estimate $i_0 \sim e^{V_c}$ follows, which shows that the stationary flow of probability grows exponentially as the height of barrier (11) of the effective potential (10) increases.

The stationary distribution function $w(f)$ is determined by Eq. (17), according to which $w(f) \approx w_0(f)$ at $f < f_c$, and $w(f) \ll w_0(f)$ in the supercritical region $f \gg f_c$. Applying equalities (17), (15), and (10), we obtain the expression

$$w(f) = i_0 \exp \left(\frac{f^2}{2} - \frac{f^{1-\beta}}{1-\beta} \right) \times \int_{f/f_c}^{\infty} \exp \left(\frac{x^{1-\beta}}{1-\beta} - \frac{x^2}{2} \right) dx. \quad (20)$$

At $\beta = 0$, it can be simplified to the form

$$w(f) = \sqrt{\frac{e\pi}{2}} i_0 \exp \left(\frac{f^2}{2} - f \right) \operatorname{erfc} \left(\frac{f - f_c}{\sqrt{2}f_c} \right). \quad (21)$$

The form of the distribution function (20) is presented in Fig. 5. The figure shows that $w(f)$ monotonously falls down within an interval determined by the critical

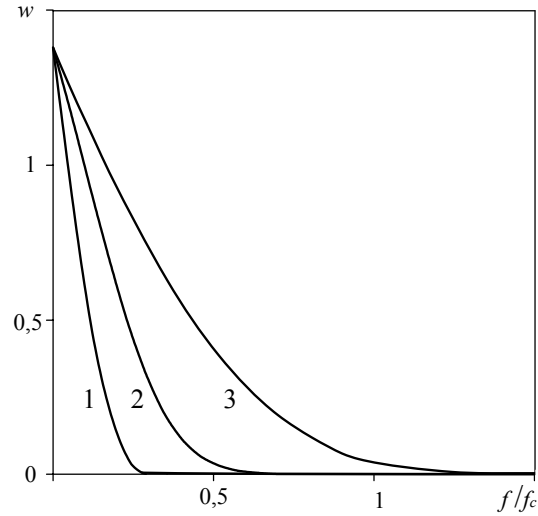


Fig. 5. Stationary distribution functions of hierarchical clusters over the thermodynamic effect values for $\beta = 0$ and $\alpha = 1.25$ (1), 1.4 (2), and 2.0 (3)

value f_c : from $w \approx 1.380$ at $f = 0$ to exponentially small values $w \ll 1$ at $f \gg f_c$, with increase in the branching index a resulting in a substantial spread of the thermodynamic effect of clustering.

At last, let us determine the critical value of the thermodynamic effect, f_c , which is responsible for the scaling of the effective coordinate $x = f_l/f_c$ of the diffusion process (12). For this purpose, let us use the last definition in (9), in which the macroscopic flow J and the microscopic value i_0 given by equality (18) are connected by the relation $N^{(a-1)/a} i_0 = J/\alpha M$. By neglecting the hierarchical gap ($G = 0$), we arrive at the expression

$$f_c = f_0 \exp \left(\frac{1}{2} \frac{1 + \beta}{1 - \beta} \frac{a}{a - 1} \right), \quad (22)$$

where the preexponential factor $f_0 \sim 1$ cannot be determined in the framework of the applied approximation. As is seen from Fig. 6, the critical value (22) grows exponentially with a reduction of the hierarchical tree branching ($a \rightarrow 1$) and the growth of index β ($\beta \rightarrow 1$).

5. Probability of Hierarchical Condensation

Since the ensemble of hierarchically subordinate condensate nuclei is represented as a self-similar set, the distribution of the probability density $P(\varphi, s)$ over values of the thermodynamic effect of nucleus formation $\varphi = N^{-\alpha/a} F$ is a homogeneous function of the distance s in the ultrametric space [23]:

$$P(\varphi, s) = (S - s)^\alpha w(f). \quad (23)$$

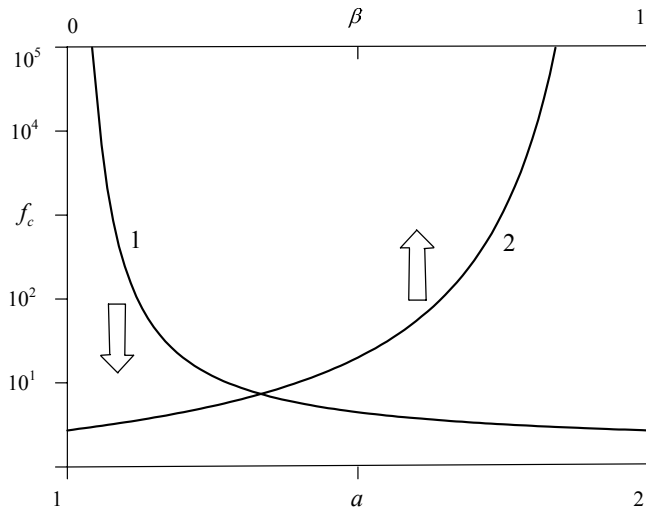


Fig. 6. Dependence of the critical value (22) on the hierarchical tree branching degree a at $\beta = 0$ (1) and on index β at $a = 2$ (2)

Hereafter, the index i of a hierarchical level is omitted, and the dependence $w(f)$ represents the stationary distribution, which was examined in the previous section. From the formal point of view, expression (23) stems from relations (6) and (1). From the physical one, it means that the total value F of the thermodynamic effect of hierarchical condensation, measured on the scale $N^{\alpha/a}$, is reduced to the share f of every nucleus. On the other hand, a decrease of the probability density (23) as the distance s in the ultrametric space grows reflects the hierarchical nature of the condensation process.

First, let us determine the probability $\bar{\mathcal{P}}(t)$ that the condensate does not nucleate before the time moment t . For this purpose, it is necessary to integrate the Debye exponential function $\exp[-t/t(s)]$ with the relaxation time $t(s) \equiv t_0 \exp[\varphi(s)]$, the magnitude of which is determined by the barrier height

$$\varphi(s) = (S - s)^{-\alpha} f(s), \tag{24}$$

which follows from equalities (6) and (1) (t_0 is the microscopic time scale), over the distance s at every time moment t . Since the indicated Debye process is realized with the probability density (23), the latter must be used as a weight function, while integrating over s . As a result, the required probability looks like

$$\bar{\mathcal{P}} = \int_0^S \exp \{ -(t/t_0) \exp [-\varphi(s)] \} P(\varphi, s) ds. \tag{25}$$

Relation (1) allows a change to the integration over the numbers of hierarchical levels l to be done. Then, the

application of equalities (23)–(25) gives rise to the expression

$$\bar{\mathcal{P}} = \int_0^S l^\alpha \exp \{ -(t/t_0) \exp [-l^{-\alpha} f(l)] \} w(f(l)) dl. \tag{26}$$

The further solution of the problem requires that the dependence $f(l)$, which is given by Eq. (8), should be determined. In the analytical form, the solution can be obtained only if $\beta = 0$, and this brings about the expression

$$f = f_c (1 + l^\alpha). \tag{27}$$

As a result, probability (26) reads

$$\bar{\mathcal{P}} = \int_{f_c}^\infty \frac{f - f_c}{f_c} \exp \left[-\frac{t}{t_0} \exp \left(-\frac{f_c f}{f - f_c} \right) \right] w(f) df, \tag{28}$$

where the distribution $w(f)$ is given by expression (21).

The simplest way to find an explicit form for dependence (26) consists in making use of the saddle-point method. The calculations (see Appendix) show that, at stages $t \gg t_{ef}$, where the scale $t_{ef} \gg t_0$ cannot be found in the framework of the applied approximation, the probability $\mathcal{P}(t) = 1 - \bar{\mathcal{P}}(t)$ of the hierarchical condensation has the asymptotic behavior

$$\mathcal{P} \simeq 1 - \frac{\sqrt{2\pi}}{\alpha} f_c^{1/\alpha} \left[\ln \left(\frac{t}{t_{ef}} \right) \right]^{-\left(\frac{1}{\alpha} + \frac{3}{2}\right)}. \tag{29}$$

Dependence (29) is valid, provided that the following conditions are obeyed.

- The inequality $f - f_c \ll f_c$ must be fulfilled. Then, the specific thermodynamic effect f can be replaced by its critical value f_c determined by equality (22). On the other hand, if $f - f_c \ll f_c$, the maximal distance S is so large ($S \gg 1$) that the continual approximation can be used.

- The probability density $w(f)$ in distribution (23) is approximated by a step function, which is equal to $w = f_c^{-1}$ within the range from 0 to f_c .

The plots of dependence (29) are shown in Fig. 7, *a*. The figure demonstrates that the probability of the hierarchical structure formation monotonously increases to the maximal value $\mathcal{P} = 1$ as the time grows. With a reduction of the hierarchical tree branching degree, when the exponent in the power-law dependence (2) acquires falling values, $a \rightarrow 1$, and the critical value (22) quickly grows, the dependence $\mathcal{P}(t)$ shifts toward longer times.

This means that a reduction of the hierarchical structure branching stimulates a reduction of the probability of its formation.

The application of expression (28), provided that distribution (21) is known, allows result (29) to be corrected with the help of the saddle-point method. The obtained time dependences of the hierarchical condensation probability are depicted in Fig. 7,*b*. The figure makes it evident that the correction is reduced to a shift of the indicated dependences toward longer times, which is equivalent to a reduction of the time scale t_{ef} . Since the character of the obtained dependences does not change at that, a conclusion can be drawn that the both methods yield qualitatively identical results.

6. Comparison Between Experimental Data and Theoretical Results

The theoretical scheme considered in Sections 3 and 4 shows that the condensate nuclei form an ensemble of subordinate objects, which are distributed over the values of thermodynamic transformation effect (6) and the distances in the ultrametric space (1), which determine the cluster dimensions. The quasiequilibrium process of condensation can be represented as the diffusive motion of a Brownian particle, which is characterized by the effective values of coordinate and time (9), over the nodes of hierarchical tree. The diffusion is described by the Langevin, Eq. (12), or the Fokker–Planck, Eq. (14), equation, which takes the external white noise (13) into account. The stationary distribution for the thermodynamic effect of condensation and the corresponding probability flow are determined by equalities (17) and (18), respectively. The behavior of the ensemble of condensate nuclei, which is determined by the homogeneous function (23), is governed by the effective potential (10), which attains its maximal value (11) at the critical value (22).

Taking the experimental situation into account, it should be noted that electron-microscopy photos presented in Fig. 1,*b* are characterized by the values of branching index in relation (2), which are not large. On the other hand, there are no physical reasons to suppose that index β of the effective mobility (4) must be large. Thus, the conditions $a - 1 \ll 1$ and $\beta = 0$ can be considered as satisfied. As a result, the critical value (22) of the specific thermodynamic effect of condensation reaches exponentially large values $f_c \gg 1$ for weakly branched structures, where index (7) is small, $\alpha \ll 1$.

According to the scenario proposed, the condensation starts from the overcoming of barrier (11) of the effective

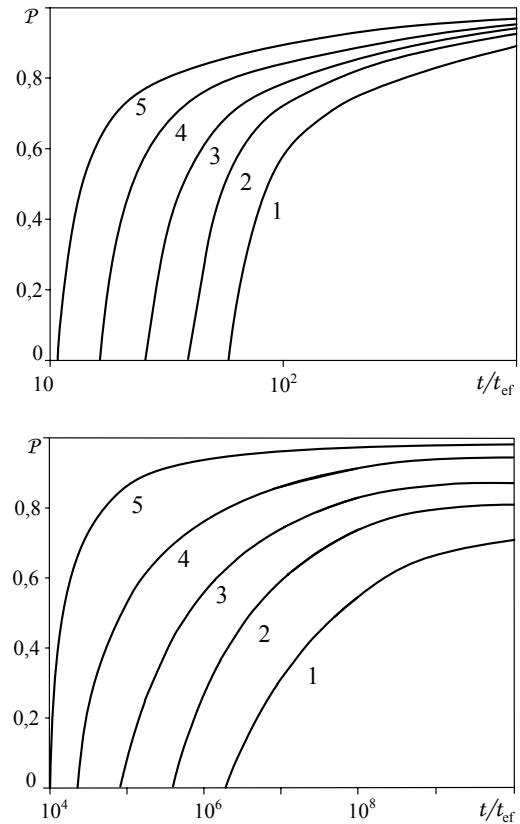


Fig. 7. Time dependences of the hierarchical condensation probability at $\beta = 0$ and various branching degrees $a = 1.40, 1.45, 1.50, 1.60,$ and 2.00 (curves 1 to 4, respectively). The upper panel demonstrates the dependences obtained by the saddle-point method, the lower one those calculated using equality (29)

potential (10), which is provided by the condition $f > f_c$ during the time interval

$$t_c \approx t_0 e^{V_c}. \tag{30}$$

The further phase formation in time is connected with the reproduction of condensate nuclei. This process is reduced to the diffusion-like growth of the thermodynamic effect of condensation (24) in the ultrametric space. As a result, the long-term asymptotics for the probability of the formation of a condensate grid structure is determined by expression (29), in which the time t must be reckoned from the critical value t_c :

$$\mathcal{P} \simeq 1 - \frac{\sqrt{2\pi}}{\alpha} f_c^{1/\alpha} \left(\ln \frac{t - t_c}{t_{ef}} \right)^{-\left(\frac{1}{\alpha} + \frac{3}{2}\right)}. \tag{31}$$

To within the substitution of t by $t - t_c$, Fig. 7,*a* exhibits the time dependences $\mathcal{P}(t)$ corresponding to various values of the hierarchical structure branching degree a . In

the previous section, it was shown that the correction of result (31), which is based on the saddle-point method, can be obtained by using expressions (28) and (21). As a result, the time dependences depicted in Fig. 7, *b* are realized. A comparison between Fig. 7, *a* and *b* testifies that this correction is reduced to a reduction of the time scale t_{ef} .

According to Fig. 7, the probability of the grid structure formation in the condensate monotonously grows in time, shifting toward longer times at a reduction of the structure branching degree. This allows us to explain the behavior of copper condensates, which can be observed on the electron-microscopy patterns depicted in Fig. 1. Really, Fig. 7 shows that, at short times of sputtering, the most probable is the formation of a cluster structure that is characterizes by an enhanced branching degree. Just such a behavior is displayed in Fig. 1, *a*, where compact condensate clusters are observed. According to Fig. 7, as the sputtering time grows, the probability of the formation of a weakly branched structure becomes appreciable. In Fig. 1, *b*, where the formation of a developed grid structure is observed, this conclusion is confirmed.

APPENDIX

Determination of the Hierarchical Condensation Probability Using the Saddle-Point Method

The saddle-point method is used for the estimation of integrals of the form

$$\mathcal{I} = \int_0^{\infty} \exp[-\phi(x)] dx, \quad (32)$$

where the function $\phi(x)$ has a narrow minimum at the point x_m . In this case, it can be approximated by the parabola

$$\phi(x) \simeq \phi_m + \frac{\phi_m''}{2} (x - x_m)^2, \quad (33)$$

where the notations

$$\phi(x_m) \equiv \phi_m, \quad \phi'(x_m) = 0, \quad \phi_m'' \equiv \phi''(x_m) \quad (34)$$

are used, and the prime means the differentiation with respect to x . The substitution of Eq. (33) into Eq. (32) brings about the result

$$\mathcal{I} \simeq \sqrt{\frac{\pi}{2\phi_m''}} e^{-\phi_m}, \quad (35)$$

provided that the minimum point is located not far from the coordinate origin ($x_m \ll 1$). In the inverse case $x_m \gg 1$, result (35) must be doubled.

In the framework of the condensation problem, the function $\phi(x)$ looks like

$$\phi(l) = \tau \exp(-fl^{-\alpha}) + \ln(l^{-\alpha}), \quad (36)$$

where the short notation $\tau \equiv t/t_0$ is introduced. The condition for dependence (36) to have an extremum is expressed by the transcendental equation

$$\exp(fl_m^{-\alpha}) = \tau (fl_m^{-\alpha}), \quad (37)$$

in which $\tau, fl_m^{-\alpha} \gg 1$. Taking the logarithm of both sides in condition (37), we obtain

$$fl_m^{-\alpha} = \ln[\tau (fl_m^{-\alpha})] \simeq \ln(C\tau), \quad (38)$$

where the last estimate is justified by the fact that the change of the variable $fl_m^{-\alpha}$ by a constant C results in an insignificant logarithmic error. As a result, the extreme value of the argument in function (36) is evaluated by the relations

$$l_m \simeq [f^{-1} \ln(C\tau)]^{-1/\alpha} \sim f_c^{1/\alpha}. \quad (39)$$

Substituting the extreme values of function (36),

$$\phi_m = f^{-1} l_m^\alpha - \ln(l_m^\alpha), \quad (40)$$

and its curvature,

$$\phi_m'' = \alpha^2 l_m^{-2} (fl_m^{-\alpha} - 1), \quad (41)$$

into equality (35), we obtain the expression

$$\bar{\mathcal{P}}(t) \simeq w(f(l_m)) \frac{l_m^{\alpha+1}}{\alpha} \sqrt{\frac{\pi/2}{fl_m^{-\alpha} - 1}} \exp(-f^{-1} l_m^\alpha) \quad (42)$$

for probability (26), where relation (27) is taken into account. Evaluating the probability density as the reciprocal critical value f_c , $w(f(l_m)) \sim 1/f_c$, we obtain

$$w(f(l_m)) l_m^{\alpha+1} \sim f_c^{1/\alpha} [\ln(C\tau)]^{-\frac{\alpha+1}{\alpha}}, \quad (43)$$

$$fl_m^{-\alpha} - 1 \sim \ln(C\tau), \quad \exp(-f^{-1} l_m^\alpha) \sim 1.$$

As a result, probability (42) looks like

$$\bar{\mathcal{P}}(t) \sim \frac{\sqrt{\pi/2}}{\alpha} f_c^{1/\alpha} [\ln(C\tau)]^{-(\frac{1}{\alpha} + \frac{3}{2})} \quad (44)$$

Redesignating the quantity $C\tau \equiv t/(C^{-1}t_0)$ as t/t_{ef} , we obtain ultimate expression (29).

1. H.E. Cook, *Acta Metall.* **23**, 1027 (1975).
2. A.J. Bray, *Adv. Phys.* **43**, 357 (1994).
3. A.I. Olemskoi, *Theory of Structure Transformations in Non-Equilibrium Condensed Matter* (NOVA Science, New York, 1999).
4. I.M. Lifshitz and V.V. Slyozov, *Zh. Éksp. Teor. Fiz.* **35**, 2 (1958).
5. A.I. Olemskoi and A.V. Paripsky, *Izv. Vyssh. Ucheb. Zaved. Fiz.* **11**, 122 (1978).
6. C. Dupas, P. Houdy, and M. Lahmani, *Nanoscience: Nanotechnologies and Nanophysics* (Springer, Berlin, 2007).
7. V.I. Perekrestov, A.S. Korniyushchenko, and Yu.A. Kosminskaya, *Pis'ma Zh. Tekh. Fiz.* **32**, 1 (2005).
8. V.I. Perekrestov, A.S. Korniyushchenko, and Yu.A. Kosminskaya, *Fiz. Tverd. Tela* **50**, 1357 (2008).

9. V.I. Perekrestov, A.S. Korniyushchenko, and Yu.A. Kosminskaya, *Pis'ma Zh. Tekh. Fiz.* **53**, 1364 (2008).
10. V.I. Perekrestov, A.I. Olemskoi, A.S. Korniyushchenko, and Yu.A. Kosminskaya, *Fiz. Tverd. Tela* **51**, 1003 (2009).
11. V.I. Perekrestov, A.I. Olemskoi, Yu.O. Kosminska, and A.A. Mokrenko, *Phys. Lett. A* **373**, 3386 (2009).
12. A.I. Olemskoi, V.I. Perekrestov, Yu.O. Kosminska, O.V. Yushchenko, A.S. Korniyushchenko, and T.I. Zhilenko, unpublished.
13. L.I. Maissel and R. Glang, *Handbook of Thin Film Technology, Vol. 1* (McGraw-Hill, New York, 1970).
14. B.S. Danilin, *Application of Low-Temperature Plasma for Thin Film Deposition* (Energoatomizdat, Moscow, 1989) (in Russian).
15. J. Feder, *Fractals* (Plenum Press, New York, 1988).
16. V.I. Perekrestov and S.N. Kravchenko, *Instrum. Eksp. Metody* **45**, 404 (2002).
17. R. Rammal, G. Thoulouse, and M.A. Virasoro, *Rev. Mod. Phys.* **58**, 765 (1986).
18. A.I. Olemskoi and A.D. Kiselev, *Phys. Lett. A* **247**, 221 (1998).
19. D.O. Kharchenko and A.V. Dvornichenko, *Eur. Phys. J. B* **61**, 95 (2008).
20. H. Risken, *The Fokker-Planck Equation* (Springer, Berlin, 1984).
21. E.M. Lifshitz and L.P. Pitaevskii, *Physical Kinetics* (Pergamon Press, Oxford, UK, 1981).
22. M. Parzusi, S. Maslov, and P. Bak, *Phys. Rev. E* **53**, 414 (1996).
23. D. Sornette, *Critical Phenomena in Natural Sciences* (Springer, New York, 2001).

Received 04.01.11.

Translated from Ukrainian by O.I. Voitenko

ДОСЛІДЖЕННЯ УМОВ ІЄРАРХІЧНОЇ КОНДЕНСАЦІЇ
ПОБЛИЗУ ФАЗОВОЇ РІВНОВАГИ

O.I. Олемскої, O.B. Ющенко, T.I. Жиленко

Резюме

Запропоновано новий механізм утворення фази, який досліджується експериментально і теоретично на прикладі квазірівноважної стаціонарної конденсації в іонно-плазмовому розпилювачі. Отримано конденсати міді, які показують, що під час наплення реалізується режим самозбирання, результатом якого є характерна сітчаста структура. Отримана при цьому фрактальна картина розподілу зародків конденсату на поверхні підкладки нагадує картину, що спостерігається у процесі утворення фази, обмеженому дифузією. Показано, що зародки конденсату формують статистичний ансамбль ієрархічно супідпорядкованих об'єктів, розподілених в ультраметричному просторі. Для опису цього ансамблю знайдено рівняння Ланжевена і Фоккера–Планка, які дозволяють визначити стаціонарний розподіл значень термодинамічного ефекту конденсації і відповідний потік імовірності. Отримано часові залежності імовірності формування розгалуженої структури конденсату, використання яких дозволяє пояснити формування сітчастої структури.